공학석사학위논문

Nanoparticle coating on silane modified surface of magnesium for local drug delivery and controlled corrosion

국소 약물 전달과 부식 제어의 구현을 위한 실레인 표면 처리된 마그네슘에 대한 나노파티클 코팅 기술의 개발

2015년 2월

서울대학교 대학원

협동과정 바이오엔지니어링전공

이 원 석

Nanoparticle coating on silane modified surface

of magnesium for local drug delivery

and controlled corrosion

국소 약물 전달과 부식 제어의 구현을 위한

실레인 표면 처리된 마그네슘에 대한

나노파티클 코팅 기술의 개발

지도교수 최 영 빈

이 논문을 공학석사 학위논문으로 제출함

2014년 12월

서울대학교 대학원

협동과정 바이오엔지니어링전공

이 원 석

이원석의 석사학위논문을 인준함

2015년 2월

위 원 장 _____ (인)

부위원장 _____ (인)

위 원 _____ (인)

Abstract

Nanoparticle coating on silane modified surface of magnesium for local drug delivery and controlled corrosion

Won Seok Lee

Interdisciplinary Program in Bioengineering,

College of Engineering,

The Graduate School

Seoul National University

In this study, we proposed a potential method for the preparation of a magnesium (Mg)-based medical device for local drug delivery and controlled corrosion. A Mg surface was modified with 3-aminopropyltrimethoxy silane, and the resulting surface was then coated with drug loaded nanoparticles made of poly (lactic-co-glycolic acid) (PLGA) via electrophoretic deposition (EPD). The drug-loaded nanoparticles (i.e., Tr_NP) exhibited a size of 250 ± 67 nm and a negative zeta potential of -20.9 ± 2.75 mV. The drug was released from the nanoparticles in a sustained manner for 21 days, and this did not

change after their coating on the silane-modified Mg. The silane-modified surface suppressed Mg corrosion. When immersed in phosphate buffered saline (PBS) at pH 7.4, the average rate of hydrogen gas generation was 0.41 - 0.45 ml/cm^2/day, compared to 0.58 - 0.6 ml/cm^2 /day from a bare Mg surface. This corrosion profile was not significantly changed after nanoparticle coating under the conditions employed in this work. The *in vitro* cell test revealed that the drug released from the coating was effective during the whole release period of 21 days, and both the silane-modified surface and carrier nanoparticles herein were not cytotoxic.

Keywords : coating; corrosion; drug delivery; magnesium; nanoparticles; silane

Student Number **:** 2013-21039

Contents

List of Figures

List of Tables

Ⅰ. Introduction

1.1. Magnesium (Mg) materials and local drug delivery

Magnesium (Mg) and Mg alloys have attracted a great deal of attention as candidate materials for implantable medical devices [1,2]. Due to their mechanical properties similar to those of natural bone, Mg and its alloys have been extensively studied for use in bone fixation systems [3,4]. More importantly, Mg-based devices can be degraded by corrosion in body fluids into Mg ions, which are metabolites already present in the body, eliminating the need for secondary removal surgery [2-4]. Mg-based devices, when functionalized with local drug delivery, can be even more beneficial as a low concentration of purposed drug can resolve local complications around the device to a large extent [5]. Therefore, this strategy has already been applied to various implantable devices, such as cardiovascular stents [6,7], orthopedic implants [8,9], and venous catheters [10,11].

The surface of the device was generally coated or modified to enable local drug delivery [12]. However, surface treatment in an aqueous environment may not be easily applicable to Mg-based devices due to the relatively fast corrosion of Mg, leading to rapid loss of mechanical strength [4]. This rapid corrosion could be problematic even after

implantation; a high concentration of hydrogen gas, generated by Mg corrosion, can accumulate near the implantation site, potentially damaging the surrounding tissues [5]. In a non-aqueous solvent, the drug-loaded polymer coating could be prepared, but the coating would not be stable due to the inherently poor adhesion between Mg and the polymer [2,13].

1.2. Strategy

In this study, we propose a potential method to prepare a Mg-based device incorporating local drug delivery. The surface of the Mg-based device was first modified with a hydrophobic water-protective layer that was then coated with drug-loaded polymeric nanoparticles. In this way, the hydrophobic layer could control Mg corrosion while coated with the drug-loaded nanoparticles and exposed to body fluid. The drug-loaded nanoparticles could be separately prepared to modulate drug release and subsequently coated onto the modified surface of Mg. The hydrophobicity of the modified surface would allow better adherence of the polymeric nanoparticles [14,15].

For this, we first prepared the silane-modified surface on a coin-shaped sample of pure Mg because of its well-known anti-corrosive effect on Mg [16,17]. The silanol groups (Si-OH) can be attached to the hydrated metal surfaces (Metal-OH), forming Si-O-metal bonds [5,18]. Then, the

silanol groups are self-cross-linked to form siloxane bonds (Si-O-Si), giving a water-protective layer chemically bound to the Mg surface [18]. We also prepared the drug-loaded nanoparticles made of poly (lactic-co-glycolic acid) (PLGA), which have been already widely used as drug carriers with high biocompatibility [19,20]. For local drug delivery, the nanoparticles were coated on the silane-modified Mg surface via electrophoretic deposition (EPD); by applying an electrical field, the charged nanoparticles in an aqueous suspension could move to the oppositely charged Mg substrate to form a relatively uniform and dense coating layer [5]. The EPD method was reported to be a rapid, economic coating process with high reproducibility compared to other conventional techniques such as spraying and dipping processes [20]. In this work, we employed tranilast as a potential drug for local delivery around the implantable device. Tranilast can inhibit abnormal fibroblast proliferation and collagen synthesis [21,22] that can be problematic around implanted medical devices.

In this study, we assessed the surface of the noncoated and coated Mg samples with scanning electron microscopy (SEM) and energy-dispersive X-ray spectroscopy (EDS). The *in vitro* drug release and corrosion tests were performed in phosphate-buffered saline (PBS; pH 7.4) [23]. To evaluate the corrosion properties, we assessed the amount of generated hydrogen gas and observed the change in surface

morphology with SEM while the Mg sample was immersed in pH 7.4 PBS. We also conducted *in vitro* cell tests to examine the efficacy of the tranilast released from the coated Mg samples.

Ⅱ. Materials and methods

2.1. Materials

Dichloromethane (DCM), dimethylformamide (DMF), acetone, methanol, ethanol and polyvinyl alcohol (PVA) were purchased from Sigma (MO, USA). Phosphate-buffered saline (PBS; pH 7.4) was obtained from the Seoul National University Hospital Biomedical Research Institute. Poly (lactic-*co*-glycolic acid) (PLGA; 50:50, LP1001, *i.v.*= 0.38 dl•g^{-1}, average MW = 54 KDa) was obtained from Lakeshore Biomaterials (AL, USA). Tranilast was purchased from Nanjing Yuance Industry & Trade (China). 3-aminopropyltrimethoxy silane (APS) was obtained from Tokyo Chemical Industry (Japan). The coins of pure Mg, 10 mm in diameter and 1.5 mm in thickness, were a kind gift from the Center for Biomaterials, Korea Institute of Science and Technology (Seoul, Korea).

2.2. Preparation of nanoparticles

We prepared the PLGA nanoparticles with the emulsion method in this work [24]. Briefly, 100 mg PLGA or a blend of 100 mg PLGA and 10 mg tranilast were dissolved in a mixed solvent of 4.5 ml DCM and 0.5 ml acetone to prepare the blank (NP) or drug-loaded nanoparticles (Tr_NP), respectively. The mixed solution was then poured into 25 ml

of an aqueous solution of 2.0 % w/v PVA, which was then sonicated for 1 min at 100 W with a digital sonic dismembrator (Model 5, Fischer Scientific, PA, USA). After that, the resulting emulsion was stirred under reduced pressure (-12.5 psi) for 2 h before filtering using 1 μm pore filter paper (No. 53, Hyundai Micro, Korea). The resulting filtrates were centrifuged at 15000 rpm for 30 min, and after removing the supernatant, the sediment nanoparticles were freeze-dried.

2.3. Preparation of Mg samples

We prepared four different Mg samples in this work:

(1) Intact Mg coins (MC)

(2) Silane-coated Mg coins (S-MC)

(3) Tr_NP-coated Mg coins (Tr_NP-MC)

(4) Tr_NP-coated S-MC s(Tr_NP-S-MC)

To prepare the MC, the Mg coins were each polished with SiC paper of 1000 grit and 2000 grit and were then washed with distilled water and ethanol using an ultrasonic cleaner (NXCS-1200, Kodo Technical, Korea). To prepare the S-MC, we first prepared a solution by mixing APS and methanol (2:98, v/v) [25]. Then, the MC was dipped in the APS solution for 30 s and then taken out and placed in an oven at 100 ℃ for 30 min to ensure the condensation of siloxanes.

For the nanoparticle coating, we employed **t**he EPD method, as

described in Figure 1. First, we prepared an aqueous coating medium, which was a mixture of ethanol and deionized water (1:9, v/v), suspended with 0.075 % w/v Tr_NP. We used a voltage power supply (PowePac^{TM} HC, Bio-rad, USA), where a stainless steel plate (2 cm x 2 cm; 316L, Hyundai Steel, Korea) was as the cathode and the MC or the S-MC was connected as the anode to prepare the NP-MC or the NP-S-MC, respectively. The cathode and the anode were located 10 mm apart and fully immersed in the coating medium [20]. We fixed the voltage at 30 V to maintain the current at 0.1 A, and the temperature was kept at 13.3 ± 0.90 ℃. In this work, we varied the times for voltage application to 30 s, 120 s and 240 s to optimize the nanoparticle coating. Among those conditions, the one showing the most homogeneous coating under observation with scanning electron microscopy (SEM) was selected to prepare the Tr_NP-S-MC. Under the same selected conditions, we prepared the Tr_NP-MC (i.e., the intact Mg coin coated with the Tr_NP) for comparison. After coating, the sample was thoroughly washed with deionized water and dried in air.

2.4. Characterization of nanoparticles

The morphology of the nanoparticles was examined via scanning electron microscopy (SEM; 7401F, JEOL, Japan) and transmission electron microscopy (TEM, JEM-1400, JEOL, Japan). For the SEM, the nanoparticles were placed on the sample mount and sputter coated with platinum for 10 min (208 HR, Cressington Scientific, England). The TEM sample was prepared by placing the nanoparticles on a copper grid. The X-ray diffraction patterns of the nanoparticles were examined and compared with those of the tranilast and PLGA, both in intact form, using an X-ray diffractometer (D/MAXRINT 2200-Ultima, Rigaku, Japan) equipped with Ni-filtered Cu Kα radiation (λ = 1.5418 Å). The samples were mounted on a glass substrate, scanned at the tube voltage and the current of 40 kV and 30 mA, respectively. The size and zeta potential of the NP and Tr_NP were examined with a zetasizer (Nano ZS analyzer, Malvern Instrument, France) while suspended in deionized water. To assess the amount of drug encapsulated in the nanoparticles, the Tr_NP was fully dissolved in DMF, which was then measured spectrophotometrically at 331 nm using a UV-Vis spectrophotometer (UV-1800, SHIMADZU, Japan). The drug encapsulation efficiency (EE) was then determined by the following equation:

$$\text{Encapsulation Efficiency (EE)} = \frac{Actual\ drug\ loading\ amount\ in\ nanoparticles}{Initial\ drug\ loading\ amount\ in\ nanoparticles} X\ 100\ (\%)$$

2.5. Evaluation of Mg samples

The surface morphology of the Mg samples herein was examined using SEM (7401F, JEOL, Japan). The elemental composition of the surface was evaluated via energy dispersive spectroscopy (EDS; Oxford INCAFETx3, JEOL, Japan) equipped with SEM. To examine the amount of tranilast in the coating, the Tr_NP-MC or Tr_NP-S-MC was immersed in DMF to fully dissolve the Tr_NP, and the resulting solution was measured spectrophotometrically at 311 nm (UV-1800, SHIMADZU, Japan).

2.6. *In vitro* drug release study

We performed *in vitro* drug release experiments with the Tr_NP and the Tr_NP-coated Mg samples (i.e., the Tr_NP-MC and Tr_NP-S-MC). For this, 2 mg Tr_NP or its coated Mg sample was placed in 100 ml or 30 ml of pH 7.4 PBS at 37 ℃, respectively while continuously stirred at 125 rpm in a shaking incubator (SI-600R, Jeio Tech, Korea). At scheduled times, a 1 ml aliquot was collected, and the same amount of fresh PBS was added back. The aliquot was then filtered with a 100 nm-pore filter membrane (6784-2501, Whatman, UK), and the resulting

sample was measured at 331 nm using a UV-vis spectrophotometer (UV-1800, SHIMADZU, Japan).

2.7. *In vitro* corrosion test

To examine the corrosion properties, the Mg samples prepared in this work were each fully immersed in 500 ml of pH 7.4 PBS at 37 ℃ (see Figure A1 in the Appendix). At scheduled times for 21 days, the volume of hydrogen gas was measured and calculated to give the generated hydrogen gas volume per unit exposed area of Mg sample [26], and the surface morphology was monitored with SEM, as described above. During the test, the PBS was fully replaced with fresh saline every day. More than three samples were tested for each sample type.

2.8. *In vitro* cell test

We used the L929 mouse fibroblast cell line (Korean Cell Line Bank, Korea) to perform the *in vitro* cell test. The L929 cells were cultured in RPMI 1640 (WelGENE, Korea) containing 10 % fetal bovine serum (FBS; Gibco, Life Technologies, UK) and 1 % antibiotics (streptomycin, 10,000 μg ml^{-1} and penicillin, 10,000 U ml^{-1}; Gibco, Life Technologies, UK).

We performed the extraction method[27] to examine the efficacy of the

tranilast released from the coating. Thus, the NP-S-MC was placed in 30 ml of pH 7.4 PBS at 37 ℃ while continuously stirred at 125 rpm in a shaking incubator (SI-600R, Jeio Tech, Korea). For this evaluation, we prepared S-MCs coated with blank NP (i.e., NP-S-MC) and tested them under the same conditions for comparison. At scheduled times, a 1 ml aliquot was extracted, and the same amount of fresh PBS was added back. Then, the L929 cells were prepared at a density of 1×10^4 cells per well in a 96-well plate and incubated for 24 h at 37 ℃ with 5 % CO_2 in a humidified atmosphere (HERAcell 150i, Thermo Scientific, USA). In each well, 100 μl of the culture medium was replaced with an equal volume of the extracted aliquot. The wells were also treated with fresh PBS and 1 % Triton X-100 (Sigma-Aldrich, USA) for the positive and negative controls, respectively. After that, the cells were incubated for another 24 h. The cell viability was evaluated using an EZ-Cytox Cell Viability Assay kit (Daeil Lab Service, Korea), following the manufacturer's instructions. Absorbance from each well was measured at 460 nm using an ELISA reader (VersaMax ELISA Microplate Reader, Molecular Devices, USA). At least five samples for each sample type were measured for statistical analysis.

2.9. Statistical analysis

The mean absorbance values from the *in vitro* cell test were analyzed by performing an analysis of variance (ANOVA) followed by Tukey's post-hoc pairwise comparison (Statistical Package for the Social Sciences (SPSS), version 19, USA), where * $p < 0.05$ was considered to be statistically significant.

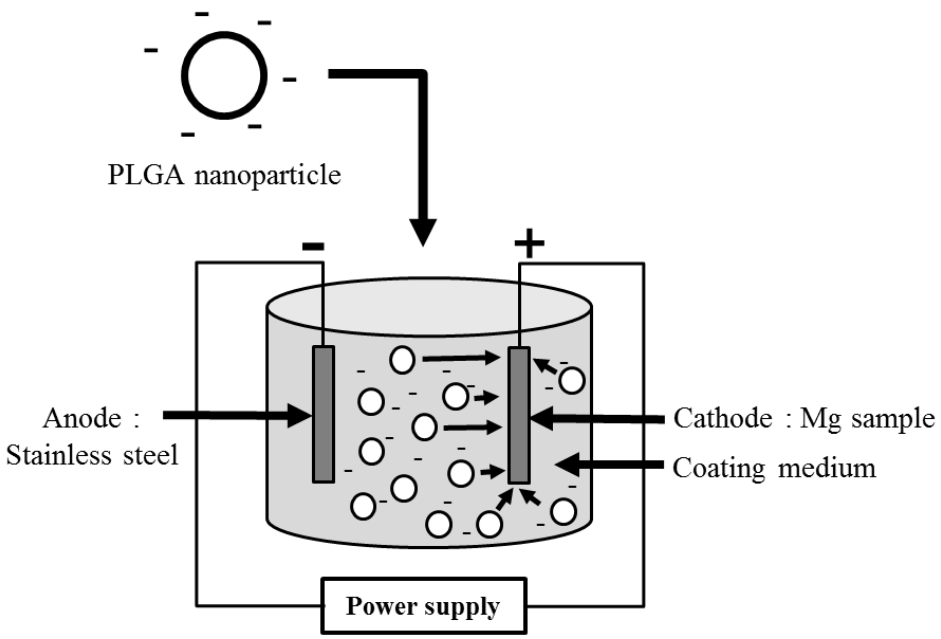

Figure 1. Schematic procedure for coating the tranilast-loaded PLGA nanoparticles on intact and silane-modified Mg coins via the EPD method.

Ⅲ. Results

3.1. Characterization of nanoparticles

According to a zetasizer analysis, the sizes of the NP and Tr_NP were measured to be 247 ± 86.2 nm and 250 ± 67.7 nm, respectively, showing negative surface charges of -24.1 ± 4.68 mV and - 28.9 ± 2.75 mV, respectively (Table 1 and Figure 2). The SEM and TEM images in Figure 3 further confirm the sizes of both the NP and Tr_NP, which were of spherical shape. For the Tr_NP, the encapsulation efficiency was 52.5 ± 5.68 %, indicating an actual loading of 90.5 ± 10.2 μg drug per mg nanoparticles. Figure 4 shows the XRD patterns of intact tranilast, intact PLGA, NP and Tr_NP. Due to its crystalline structure, tranilast exhibited characteristic XRD peaks [28], whereas no characteristic peaks were observed in the intact PLGA and NP due to their amorphous structures [29]. Notably, the characteristic peaks of tranilast were not observable with the Tr_NP, implying that the drug was distributed at the molecular level without forming crystalline regions in the nanoparticles.

Sample	Particle size (nm)	Zeta potential (mV)
NP	247 ± 86.2	-24.1 ± 4.68
Tr_NP	250 ± 67.7	-20.9 ± 2.75

Table 1. Properties of blank and tranilast-loaded nanoparticles.

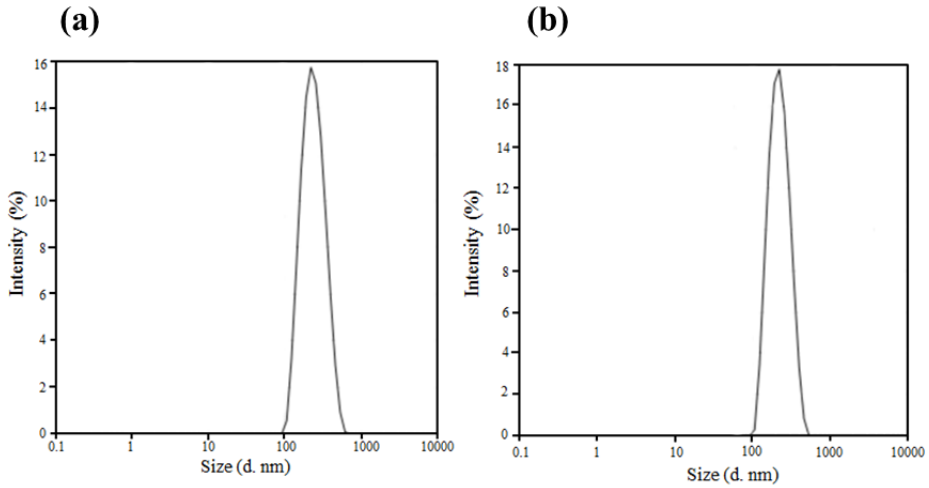

Figure 2. Size distributions of (a) NP and (b) Tr_NP.

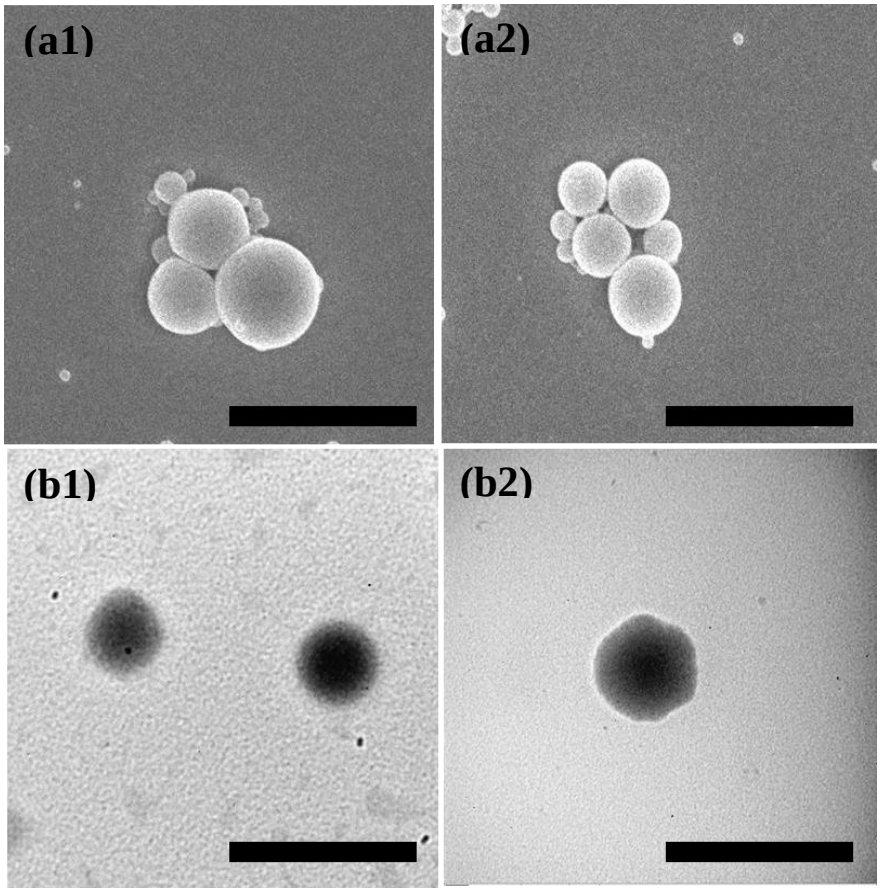

Figure 3. Nanoparticle morphologies from electron microscopy. The SEM images of (a1) NP and (a2) Tr_NP. The TEM images of (b1) NP and (b2) Tr_NP. The scale bars are 500 nm.

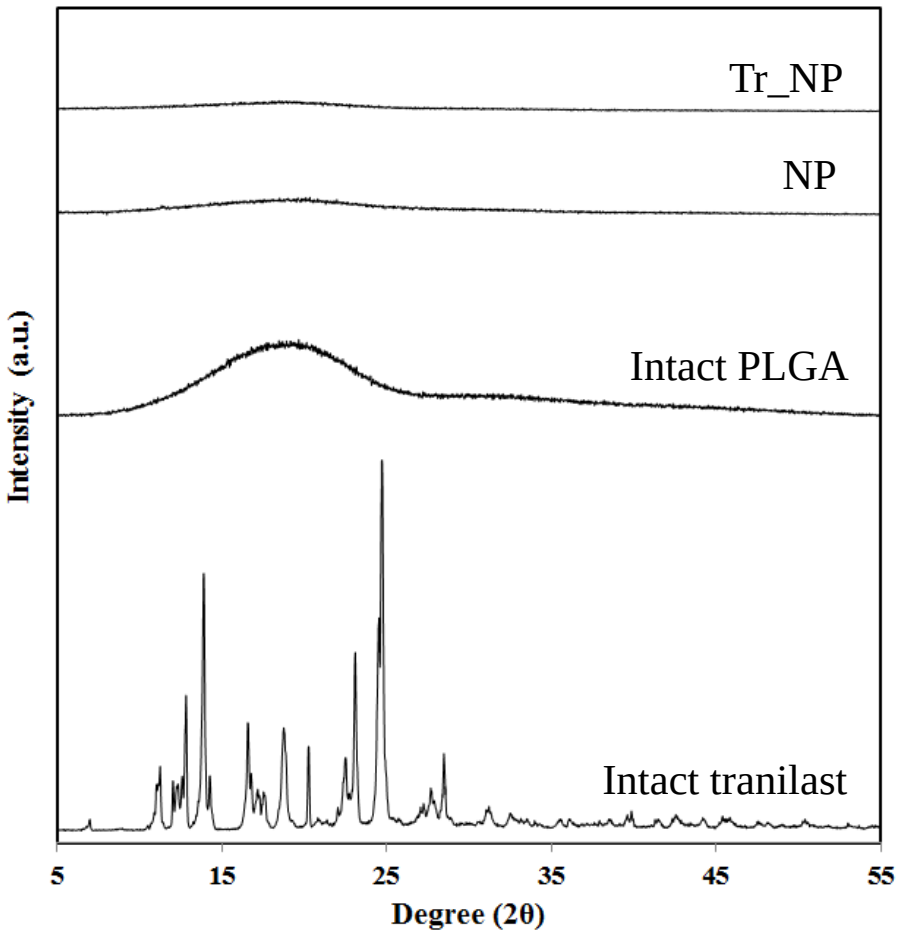

Figure 4. XRD patterns of intact tranilast, intact PLGA, NP, and Tr_NP.

3.2. Characterization of coatings

In this work, to modulate the corrosion of Mg, we prepared a silane-modified surface with intact Mg coins to produce S-MC. According to the SEM images in Figure 5, the surface of the MC showed a smooth surface with almost no micro-defects after polishing, and this surface morphology appeared to be well retained within the S-MC. The EDS analysis revealed that Mg and O were present on the surface of the MC, ascribed to the formation of the oxide layer [2]. In contrast, the S-MC showed the presence of Si in addition to Mg and O, implying the formation of a silane-modified surface (Figure 5(b)).

To coat the Tr_NP, we conducted the EPD process with the S-MC (Figure 1), where the coating conditions (i.e., the time for voltage application) were first varied for optimization. Figure 6 shows the surface morphologies of the coated S-MC under those varying conditions. As the time for the voltage application increased, more nanoparticles were observed to adhere to the surface of the S-MC. However, with a long time EPD of 240 s, the Tr_NP were observed to be deposited, forming agglomerates (Figure 6(c)). Meanwhile, when the application time was short (30 s), many areas on the surface were observed to be non-deposited (Figure 6(a)). In this work, we found that the Tr_NP could be almost homogeneously deposited when the EPD was performed for 120 s (Figure 6(b)). Under this fixed condition,

therefore, we prepared the Tr_NP-S-MC, as well as the Tr_NP-MC. The drug-loading amounts in the resulting Tr_NP-S-MC and Tr_NP-MC were measured to be 256.8 ± 75.6 μg and 243.2 ± 41.2 μg, respectively.

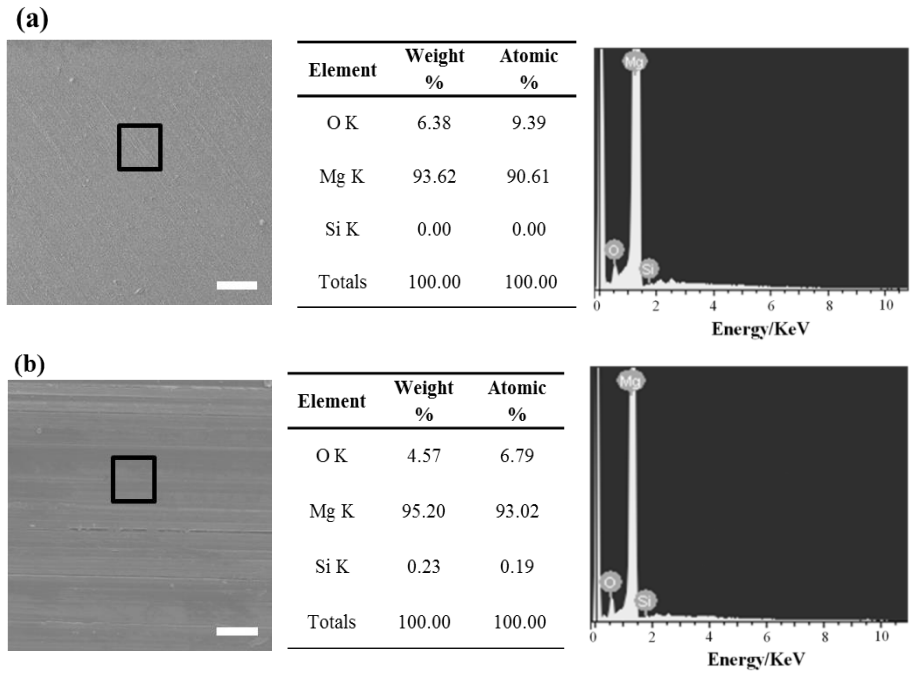

Figure 5. SEM images and EDS data obtained from (a) MC and (b) S-MC. The scale bars are 100 μm.

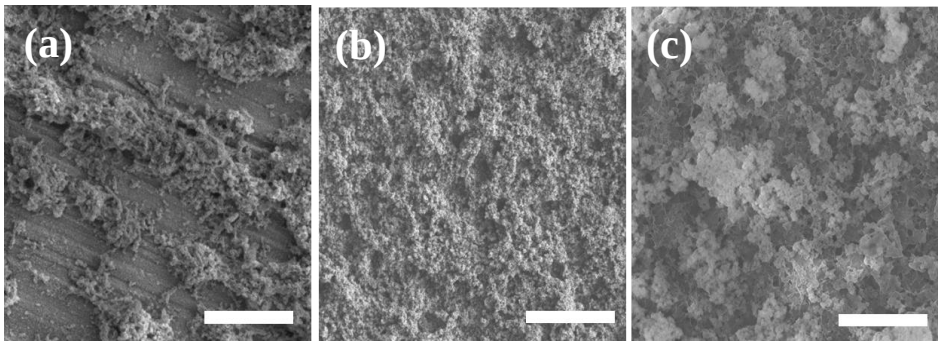

Figure 6. SEM images of the Tr_NP coated S-MC prepared under varying conditions of EPD. The voltage was fixed at 30 V and its application times were varied to (a) 30 s, (b) 120 s and (c) 240 s. The scale bars are 10 μm.

3.3. *In vitro* drug release profile

We performed the *in vitro* drug release test with the Tr_NP, Tr_NP-MC and Tr_NP-S-MC in pH 7.4 PBS at 37 ℃. As shown in Figure 7, for all samples, drug release was sustained for approximately 20 days. All exhibited a burst release on the first day, which was approximately 56 – 61 %. Notably, the drug release profiles of the coated Mg samples (i.e., Tr_NP-MC and Tr_NP-S-MC) were not very different from each other, and they were rather similar to the release profile of the Tr_NP alone, i.e., the drug-loaded nanoparticles themselves. This result indicates that the sustained drug release capacity of the Tr_NP could be well retained even after coating on the Mg surface.

.

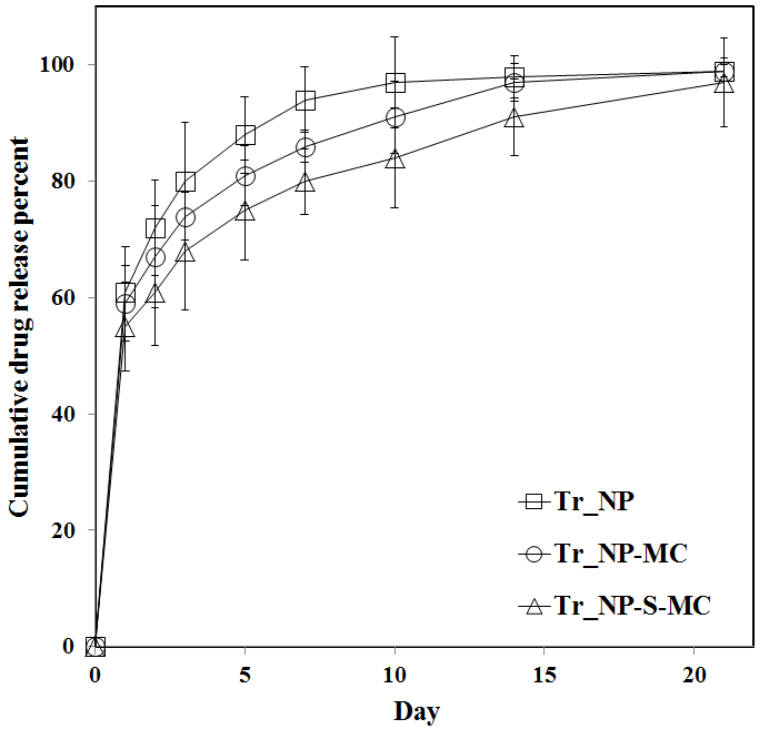

Figure 7. *In vitro* release profile of tranilast from the the Tr_NP, Tr_NP-MC and Tr_NP-S-MC.

3.4. *In vitro* Mg corrosion property

To evaluate the corrosion rate of the Mg samples, we conducted an *in vitro* immersion test in pH 7.4 PBS 37 ℃. For this, we first evaluated the volume of generated hydrogen gas [26], as shown in Figure 8. For all Mg samples herein, the total volume of generated hydrogen gas increased as the time elapsed. However, it was apparent that the rate of corrosion was influenced mostly by the surface modification with silane. The corrosion was slower with the S-MC and Tr_NP-S-MC than with the Mg samples without silane modification, i.e., the MC and Tr_NP-MC. Thus, for the S-MC and Tr_NP-S-MC, the rates of hydrogen gas generation were 0.45 and 0.41 ml/cm^2/day, respectively, which increased to 0.58 and 0.6 ml/cm^2/day for the MC and Tr_NP-MC, respectively. The coating of the nanoparticles did not seem to influence the corrosion rate much. This result indicated that the silane-modified surface indeed prevented water permeation, slowing corrosion [25].

We also examined the surface morphology of the Mg samples during *in vitro* corrosion test by assessing the SEM images (Figure 9). The MC showed pits and cracks from day 1, which became larger and more discernable as time elapsed due to its rapid corrosion (Figure 9(a1-a4)). For the Tr_NP-MC, the presence of the nanoparticles was apparent on day 1, and thus the surface under them could not be observed (Figure 9(b1)). From day 5, the pits and cracks became discernible again due to

the rapid corrosion of the Mg (Figure 9(b1-b4)). This unstable surface appeared to also cause rapid detachment of the nanoparticles, many of which could not be observed from day 5 (Figure 9(b2)). In contrast, for the S-MC, i.e., with silane modification, a smooth surface was observed on day 1 (Figure 9(c1)), and the surface did not change much until day 5 (Figure 9(c2)). The pits and cracks were observable from day 10 (Figure 9(c3-c4)). For the Tr_NP-S-MC, because of its slow corrosion, the nanoparticles were well adhered to the surface until day 5 (Figure 9(d1-d2)). The corroded surface was apparent from day 10, which was similar to that observed with the S-MC.

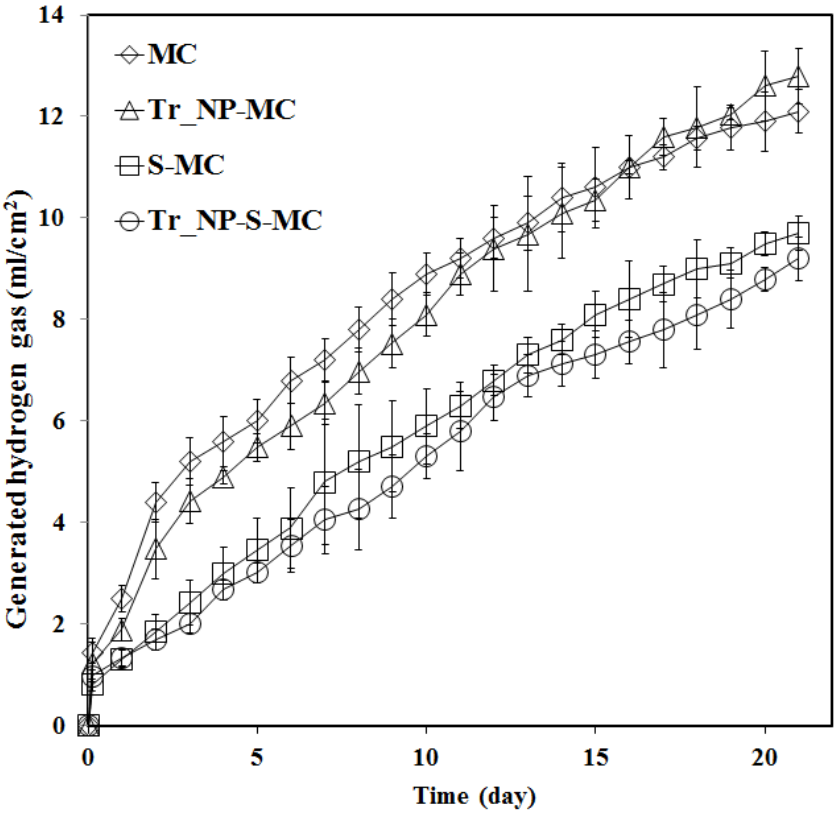

Figure 8. Volume of hydrogen gas generated from MC, Tr_NP-MC, S-MC and Tr_NP-S-MC immersed in pH 7.4 PBS at 37 ℃.

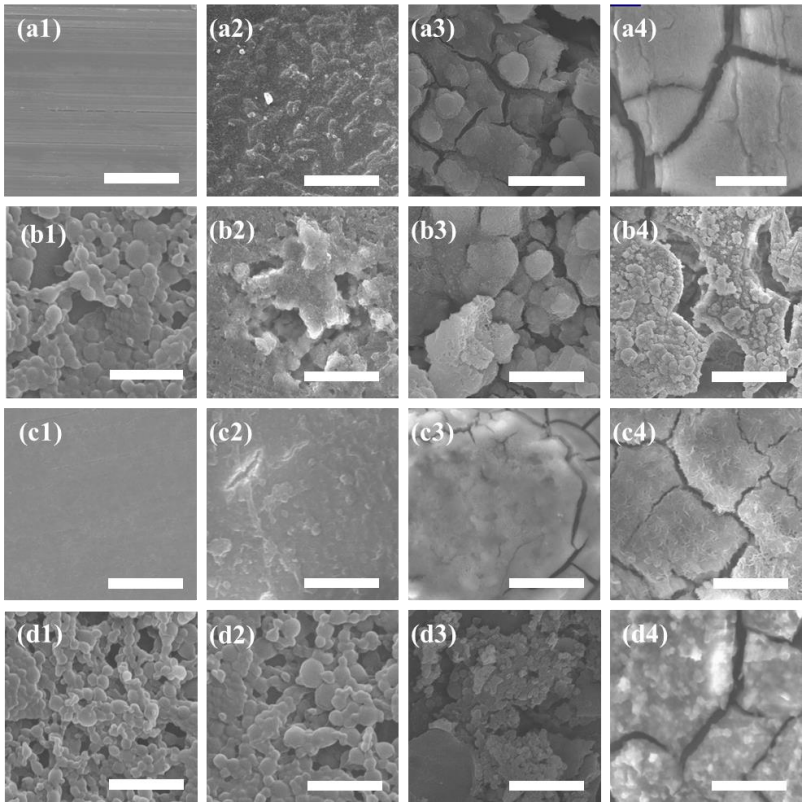

Figure 9. SEM images of the sample surfaces obtained during the corrosion test. The samples and days of imaging were (a1) MC, day 1; (a2) MC, day 5; (a3) MC, day 10; (a4) MC, day 21; (b1) Tr_NP-MC, day 1; (b2) Tr_NP-MC, day 5 ; (b3) Tr_NP-MC, day 10 ; (b4) Tr_NP-MC, day 21; (c1) S-MC, day 1; (c2) S-MC, day 5 ; (c3) S-MC, day 10 ; (c4) S-MC, day 21; (d1) Tr_NP-S-MC, day 1; (d2) Tr_NP-S-MC, day 5 ; (d3) Tr_NP-S-MC, day 10 ; (d4) Tr_NP-S-MC, day 21. The scale bars are 1 μm.

3.5. *In vitro* cell test

To examine the efficacy of the released tranilast, we preformed the extraction method [27] using L929 fibroblasts. Tranilast is known to inhibit fibroblast proliferation [30], and thus the lowered cell viability indicated the efficacy of the tranilast. As shown in Figure 10, the Tr_NP-S-MC showed significantly lower cell viability during the whole testing period of 21 days ($p < 0.05$) than that in PBS. This result confirmed the continuous drug release (Figure 7) and its retained activity. Notably, the NP-S-MC (i.e., the silane-modified Mg sample coated with the blank nanoparticles without tranilast) exhibited no significant difference in cell viability compared with that in PBS, suggesting that the carrier nanoparticles and silane-modified Mg were not cytotoxic.

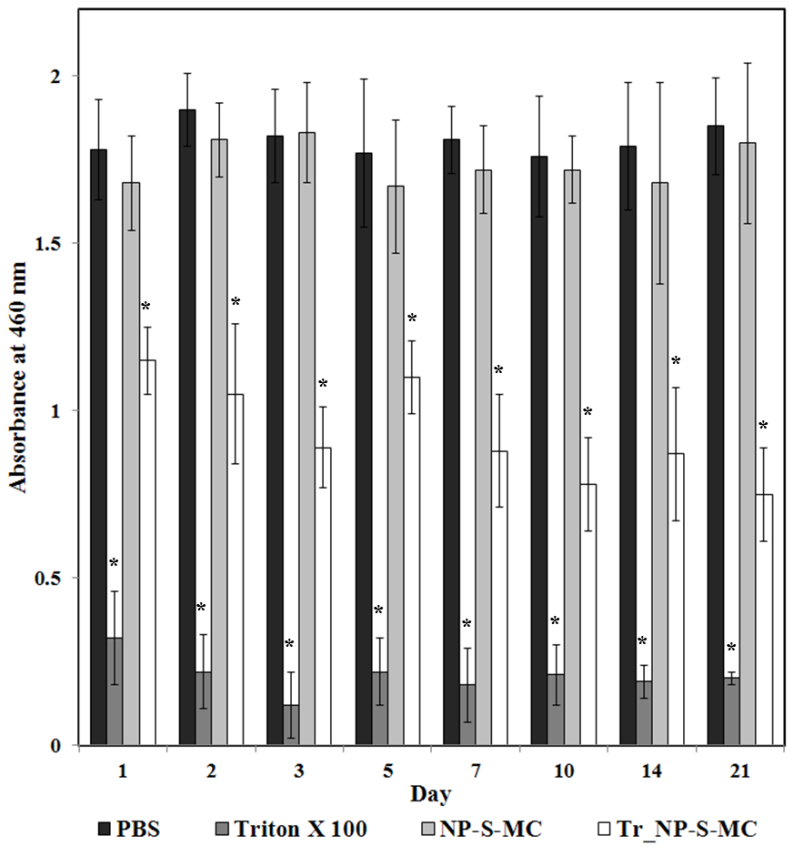

Figure 10. *In vitro* cell test evaluated by a Ez-cytox cell viability kit. (*, $p < 0.05$).

Ⅳ. Discussion

Mg and its alloys have been considered as candidate materials for implantable medical devices due to their good mechanical properties and most importantly, biodegradability [5]. However, to allow added functionalities such as local drug delivery, the surface of Mg-based devices may need to modified [31,32]. Rapid corrosion of Mg makes the processing especially difficult under an aqueous environment [4]. As a potential method to resolve this problem, we propose to first prepare a silane-modified surface on Mg, which was then coated with the drug-loaded polymeric nanoparticles. In this way, the drug-loaded nanoparticles could be separately prepared for controlled delivery, which could then be coated on Mg with the EPD method while the rapid corrosion could be prevented by the silane-modified surface.

A silane modification has been employed to treat the surface of Mg or its alloys to provide a physical barrier against water penetration [33]. In our work, a silane-modified surface of the S-MC and Tr_NP-S-MC indeed suppressed the corrosion compared with the non-coated Mg surface of the MC and Tr_NP-MC (Figures 8 and 9). It should be noted that the respective corrosion profiles did not change much even after nanoparticle coating (Figure 8). In addition, the organo-functional groups in silane could form interpenetrating networks with the reactive groups in the polymers [34,35]. Because of this, while immersed in

aqueous media, the drug-loaded nanoparticles of PLGA herein were observed to be well adhered on the surface of the Tr_NP-S-MC for a longer time than with the Tr_NP-MC (Figure 9).

Due to the carboxyl group of PLGA, the nanoparticles herein have a negative surface charge (Table 1) [20,36], which enabled the EPD method for nanoparticle coating on Mg. With PLGA serving as the drug diffusion barrier, the nanoparticles exhibited a sustained release property (Figure 7) while retaining its efficacy during the release period (Figure 10). The drug release profile of the nanoparticles did not change much even after being coated on the Mg surface (Figure 7). In addition, PLGA, a major constituent of the nanoparticles, is known to be degraded into common metabolites already found in the body, providing high biocompatibility [20]. The silane-based materials have been proven to be safe to a large extent [37,38]. Therefore, no apparent cytotoxicity was observed for the silane-modified Mg sample coated with the blank carrier nanoparticles (i.e., NP-S-MC) in this work (Figure 10).

According to our findings, a silane-modified surface of Mg was advantageous to modulate its corrosion rate. In this sense, a thicker coating or a multi-layered coating with silane would better tailor the Mg corrosion rate [5]. More hydrophobic materials, such as 1,2-bis-[triethoxysilyl] ethane (BTSE), could also be good candidates for

surface modification of Mg [39,40]. With a better water protective layer, there would be more available processing conditions to prepare a functional surface on Mg.

Ⅴ. Conclusion

For controlled corrosion and local drug delivery, we propose a silane-modified Mg surface coated with drug-loaded nanoparticles. The silane-modified surface can suppress the rapid corrosion of Mg as a hydrophobic barrier against water penetration. The drug-loaded PLGA nanoparticles can release the drug in a sustained manner with retained efficacy even after being coated on the Mg surface. We demonstrated that the drug-loaded PLGA nanoparticles could be almost homogeneously deposited on the Mg surface using the EPD method, during which the Mg corrosion could be well modulated with silane-modification. Both the silane-based surface and PLGA nanoparticles were proven to not be cytotoxic. Therefore, we conclude that a silane-modified surface coated with drug-loaded nanoparticles is a promising strategy for the preparation of Mg-based functional medical devices.

Ⅵ. References

1. Zhang S, Zhang X, Zhao C, et al. Research on an Mg-Zn alloy as a degradable biomaterial. Acta biomaterialia. 2010; 6: 626-40.
2. Park M, Lee JE, Park CG, Lee SH, Seok HK and Choy YB. Polycaprolactone coating with varying thicknesses for controlled corrosion of magnesium. Journal of Coatings Technology and Research. 2013; 10: 695-706.
3. Wang H and Shi Z. In vitro biodegradation behavior of magnesium and magnesium alloy. Journal of Biomedical Materials Research Part B: Applied Biomaterials. 2011; 98: 203-9.
4. Staiger MP, Pietak AM, Huadmai J and Dias G. Magnesium and its alloys as orthopedic biomaterials: a review. Biomaterials. 2006; 27: 1728-34.
5. Liu X, Yue Z, Romeo T, et al. Biofunctionalized anti-corrosive silane coatings for magnesium alloys. Acta biomaterialia. 2013; 9: 8671-7.
6. Schwartz RS, Chronos NA and Virmani R. Preclinical restenosis models and drug-eluting stents: still important, still much to learn. Journal of the American College of Cardiology. 2004; 44: 1373-85.
7. Tanabe K, Regar E, Lee CH, Hoye A, Giessen WJ and Serruys PW. Local drug delivery using coated stents: new developments and future perspectives. Current pharmaceutical design. 2004; 10: 357-

67.

8. Kandziora F, Bail H, Schmidmaier G, et al. Bone morphogenetic protein-2 application by a poly (D, L-lactide)-coated interbody cage: in vivo results of a new carrier for growth factors. Journal of Neurosurgery: Spine. 2002; 97: 40-8.
9. Leach JK and Mooney DJ. Bone engineering by controlled delivery of osteoinductive molecules and cells. Expert opinion on biological therapy. 2004; 4: 1015-27.
10. Darouiche RO, Smith Jr JA, Hanna H, et al. Efficacy of antimicrobial-impregnated bladder catheters in reducing catheter-associated bacteriuria: a prospective, randomized, multicenter clinical trial. Urology. 1999; 54: 976-81.
11. Richards CL, Hoffman KC, Bernhard JM, Winslow SD, Norman JC and Whalen RL. Development and characterization of an infection inhibiting urinary catheter. ASAIO journal. 2003; 49: 449-53.
12. Wu P and Grainger DW. Drug/device combinations for local drug therapies and infection prophylaxis. Biomaterials. 2006; 27: 2450-67.
13. Chen Y, Song Y, Zhang S, Li J, Zhao C and Zhang X. Interaction between a high purity magnesium surface and PCL and PLA coatings during dynamic degradation. Biomedical Materials. 2011;

6: 025005.

14. Miller A and Berg J. Effect of silane coupling agent adsorbate structure on adhesion performance with a polymeric matrix. Composites Part A: Applied Science and Manufacturing. 2003; 34: 327-32.
15. Mittal KL. Silanes and other coupling agents. CRC Press, 2007.
16. Zucchi F, Grassi V, Frignani A, Monticelli C and Trabanelli G. Influence of a silane treatment on the corrosion resistance of a WE43 magnesium alloy. Surface and coatings technology. 2006; 200: 4136-43.
17. Zucchi F, Frignani A, Grassi V, Balbo A and Trabanelli G. Organo-silane coatings for AZ31 magnesium alloy corrosion protection. Materials Chemistry and Physics. 2008; 110: 263-8.
18. Kurth DG and Bein T. Surface reactions on thin layers of silane coupling agents. Langmuir. 1993; 9: 2965-73.
19. Jawahar N, Eagappanath T, Venkatesh N, Jubie S and Samanta M. Preparation and Characterisation of PLGA-Nanoparticles containing an Anti-hypertensive agent. International Journal of PharmTech Research. 2009; 1.
20. Nam SH, Nam HY, Joo JR, Baek IS and Park J. Curcumin-loaded PLGA nanoparticles coating onto metal stent by electrophoretic deposition techniques. BULLETIN-KOREAN CHEMICAL

SOCIETY. 2007; 28: 397.

21. Wang Y and Burgess D. Drug±device combination products. Drug-Device Combination Products: Delivery Technologies and Applications. 2009: 1.
22. Suzawa H, Kikuchi S, Arai N and Koda A. The mechanism involved in the inhibitory action of tranilast on collagen biosynthesis of keloid fibroblasts. Japanese journal of pharmacology. 1992; 60: 91-6.
23. Xin Y, Hu T and Chu PK. Influence of test solutions on in vitro studies of biomedical magnesium alloys. Journal of The Electrochemical Society. 2010; 157: C238-C43.
24. Mainardes RM and Evangelista RC. PLGA nanoparticles containing praziquantel: effect of formulation variables on size distribution. International journal of pharmaceutics. 2005; 290: 137-44.
25. Zhu R, Zhang J, Chang C, Gao S and Ni N. Effect of silane and zirconia on the thermal property of cathodic electrophoretic coating on AZ31 magnesium alloy. Journal of Magnesium and Alloys. 2013; 1: 235-41.
26. Lee J-Y, Han G, Kim Y-C, et al. Effects of impurities on the biodegradation behavior of pure magnesium. Metals and Materials International. 2009; 15: 955-61.

27. Use of International Standard ISO- 110993, "Biological Evaluation of Medical Devices Part 1: Evaluation and Testing". Department of Health and Human Services, Food and Drug Administration, Center for Devices and Radiological Health, Office of Device Evaluation, 2013.
28. Kawabata Y, Yamamoto K, Debari K, Onoue S and Yamada S. Novel crystalline solid dispersion of tranilast with high photostability and improved oral bioavailability. European Journal of Pharmaceutical Sciences. 2010; 39: 256-62.
29. Xin F, Jian C, Jianming R, Zhongcheng Z and Jianpeng Z. Effects of surface modification on the properties of poly (lactide-co-glycolide) composite materials. Polymer-Plastics Technology and Engineering. 2009; 48: 658-64.
30. Darakhshan S and Pour AB. Tranilast: A review of its therapeutic applications. Pharmacological Research. 2014.
31. Witte F. The history of biodegradable magnesium implants: a review. Acta biomaterialia. 2010; 6: 1680-92.
32. Witte F, Kaese V, Haferkamp H, et al. In vivo corrosion of four magnesium alloys and the associated bone response. Biomaterials. 2005; 26: 3557-63.
33. Song J and Van Ooij WJ. Bonding and corrosion protection mechanisms of γ-APS and BTSE silane films on aluminum

substrates. Journal of Adhesion Science and Technology. 2003; 17: 2191-221.

34. Fourche G. An overview of the basic aspects of polymer adhesion. Part II: application to surface treatments. Polymer Engineering & Science. 1995; 35: 968-75.
35. Zhu D. Corrosion protection of metals by silane surface treatment. University of Cincinnati, 2005.
36. Panyam J and Labhasetwar V. Biodegradable nanoparticles for drug and gene delivery to cells and tissue. Advanced drug delivery reviews. 2003; 55: 329-47.
37. Lung CYK and Matinlinna JP. Aspects of silane coupling agents and surface conditioning in dentistry: an overview. Dental Materials. 2012; 28: 467-77.
38. Matinlinna JP, Lassila LV, ?zcan M, YliUrpo A and Vallittu PK. An introduction to silanes and their clinical applications in dentistry. International Journal of Prosthodontics. 2004; 17: 155-64.
39. Zhang J and Wu C. Corrosion protection behavior of AZ31 magnesium alloy with cathodic electrophoretic coating pretreated by silane. Progress in Organic Coatings. 2009; 66: 387-92.
40. Montemor M and Ferreira M. Electrochemical study of modified bis-[triethoxysilylpropyl] tetrasulfide silane films applied on the AZ31 Mg alloy. Electrochimica Acta. 2007; 52: 7486-95.

Ⅶ. Appendix

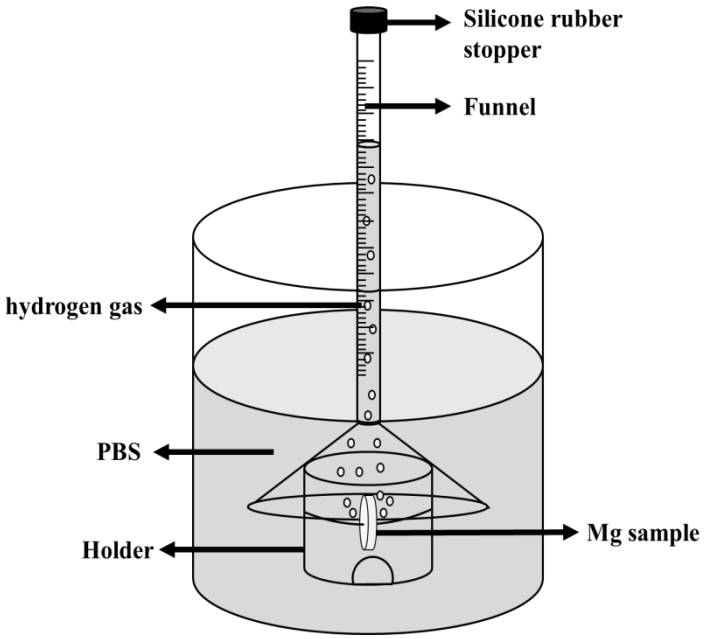

Figure A1. Schematic illustration of a funnel system to measure the volume of generated hydrogen gas during *in vitro* Mg corrosion test. The Mg sample was fully immersed in 500 ml of pH 7.4 PBS at 37 ℃.

국문초록

국소 약물 전달과 부식 제어의 구현을 위한 실레인 표면 처리된 마그네슘에 대한 나노파티클 코팅 기술의 개발

마그네슘 및 마그네슘 합금은 인체 내의 뼈와 비슷한 기계적 강도를 가지고 있으며, 시술 후 체내에서 분해되어 사라지는 특성을 가져 2차 수술이 필요 없다는 장점으로 인해 현재 골절된 뼈의 고정을 위한 의료기기의 재료 등으로 널리 사용되고 있다. 또한 표면 코팅을 통해 국소 약물 전달 기능이 부가된 마그네슘 기반의 의료기기는 국소 약물 전달을 통해 이식 후 수술 부위에서 나타날 수 있는 부작용을 해결할 수 있다는 점으로 인하여 큰 주목을 받고 있다. 하지만 체내에서 마그네슘의 과도한 부식으로 인한 기포의 발생과 그로 인한 기계적 강도의 하락, 또한 이와 더불어 마그네슘 표면과 약물이 탑재된 코팅층의 낮은 접착력은 마그네슘 기반의 의료기기에 국소 약물 전달 기능을 부여하는 것을 어렵게 만드는 단점이 있다. 이를 해결하고자 본 연구에서는 첫

번째로 부식 억제 효과를 가지는 물질인 3-아미노프로필트라이메톡실 실레인 (APS)을 코인 모양의 순마그네슘 샘플에 코팅하여 표면처리를 한 후, 두 번째로 트라닐라스트를 약물로 채택, 트라닐라스트가 탑재된 폴리(락틱-코-글리콜산) (PLGA) 고분자 기반의 나노파티클을 제작하였다. 그 후, 약물이 탑재된 나노파티클을 먼저 준비한 실레인으로 표면처리 된 마그네슘 샘플의 표면에 Electrophoretic deposition (EPD) 공정을 통하여 코팅하였다. 본 연구에서는 트라닐라스트가 탑재된 PLGA 나노파티클은 250 ± 67 nm 의 크기와 -20.9 ± 2.75 mV의 제타포텐셜을 가짐을 확인하였으며, 인 비트로 약물 방출 실험을 통해 본 연구에서 제안한 공정을 통해 코팅된 PLGA 나노파티클 코팅층으로부터 약물이 21일 동안 방출됨을 확인하였다. 또한 37 ℃의 pH 7.4 PBS 용액에 마그네슘 샘플을 침지 시킨 후 21일간의 수소 가스 발생량을 통해 실레인 표면처리의 마그네슘 부식 억제 효과를 확인한 결과 실제로 마그네슘 샘플의 부식이 억제됨을 확인하였으며, 코팅된 PLGA 나노파티클은 부식에 큰 영향을 끼치지 않음 또한 확인하였다. 세포를 이용한 인 비트로 세포실험에서는 약물이 탑재된 PLGA

나노파티클 코팅이 약물이 방출되는 21일 동안 실제적인 효능을 가짐을 증명하였고, 더불어 실레인 코팅과 약물이 탑재되지 않은 PLGA 나노파티클 코팅은 세포독성을 가지지 않음 또한 알 수 있었다. 따라서 본 연구에서 제시한 마그네슘 표면에 대한 전략인, 실레인 표면처리 및 그에 뒤따른 EPD를 통한 약물 탑재 PLGA 나노파티클의 코팅 방법은 효과적으로 마그네슘의 부식을 억제하고 국소 약물 기능을 부여할 수 있음을 증명하였다.

주 요 어 : 코팅, 부식, 약물 전달, 마그네슘, 나노파티클, 실레인

학 번 : 2013-21039